Improved AlGaInP-based red (670–690 nm) surface-emitting lasers with novel C-doped short-cavity epitaxial design

R. P. Schneider, Jr.,[a] M. Hagerott Crawford, K. D. Choquette, K. L. Lear, S. P. Kilcoyne, and J. J. Figiel
Sandia National Laboratories, Albuquerque, New Mexico 87185-0603

(Received 24 February 1995; accepted for publication 30 April 1995)

A modified epitaxial design leads to straightforward implementation of short (1λ) optical cavities and the use of C as the sole *p*-type dopant in AlGaInP/AlGaAs red vertical-cavity surface-emitting lasers (VCSELs). Red VCSELs fabricated into simple etched air posts operate continuous wave at room temperature at wavelengths between 670 and 690 nm, with a peak output power as high as 2.4 mW at 690 nm, threshold voltage of 2.2 V, and peak wallplug efficiency of 9%. These values are all significant improvements over previous results achieved in the same geometry with an extended optical cavity epitaxial design. The improved performance is due primarily to reduced optical losses and improved current constriction and dopant stability. © *1995 American Institute of Physics.*

AlGaInP materials technology has steadily advanced over the past several years, leading to high-performance edge-emitting lasers (EELs)[1] and red vertical-cavity surface-emitting lasers (VCSELs).[2,3] Relative to the AlGaInP system, AlGaAs benefits from improved index contrast, reduced electrical and thermal resistivity, a more mature processing technology, and the ability to use carbon as the *p*-type dopant for superior dopant control and stability.[4] However, integrating AlGaInP-based active regions with C-doped AlGaAs-based DBRs are made difficult by poor carrier transport into the AlGaInP active region and the inability to use C for *p*-doping in AlGaInP alloys. Previous reports of AlGaInP/AlGaAs heterostructure laser diodes have all employed Zn or Mg doping on the *p* side of the junction to improve hole injection,[5,6] eliminating a potential key advantage of the use of AlGaAs and further complicating dopant diffusion characteristics.[7,8] Such difficulties have led to implementation of relatively thick (8λ) optical cavities in red VCSELs[6] at the cost of increased optical loss and thermal resistivity and less efficient current constriction.

In the present letter we investigate a modified epitaxial design that not only enables straightforward implementation of short (1 wave) optical cavities but also the use of carbon as the sole *p*-type dopant in AlGaInP/AlGaAs-based red EELs and VCSELs. This approach better utilizes the advantages of AlGaAs materials technology in the device structure and eliminates the problems with Zn and Mg doping entirely. The resulting VCSELs benefit from considerable simplification of the growth and doping and significantly improved performance. This work also represents the first successful use of C as the only *p*-type dopant in AlGaInP-based red laser diodes.

All the devices described in this work were grown using low-pressure metalorganic vapor phase epitaxy (MOVPE) in a horizontal quartz reaction chamber as described previously.[9] The dopants include Si (from disilane) for *n*-type AlGaAs and AlGaInP, C (from CC14) for *p*-type AlGaAs(P), and Zn (from dimethylzinc) and Mg (from *bis*-cyclopentadienyl magnesium) for *p*-type AlGaInP. Several different laser heterostructures were investigated, as described. The EEL quantum well (QW) active regions contain one or three $Ga_{1-x}In_xP$ strained QWs with nominal composition $x \sim 0.56$ and thickness $L_z \sim 6-8$ nm, adjusted for photoluminescence emission between 660 and 670 nm. The barriers are composed of $(Al_{0.5}Ga_{0.5})_{0.5}In_{0.5}P$, and spacer layers of $(Al_{0.75}Ga_{0.25})_{0.5}In_{0.5}P$ are incorporated between the QW active region and the cladding layers.[6] The composition of the 0.9 μm-thick cladding layers in the EELs is either $Al_{0.5}In_{0.5}P$ or $Al_xGa_{1-x}As$ ($x \sim 0.8$). For the VCSEL structures, similar QW active regions are used, and the DBRs are composed of 0.15 wave thick AlAs and $Al_{0.5}Ga_{0.5}As$ layers separated by 0.1 wave thick continuous biparabolically graded $Al_xGa_{1-x}As$ segments to reduce series resistance.[3,9] The devices are fabricated as simple etched air posts, with postdiameters between 8–40 μm and 5–30 μm optical apertures in annular *p* contacts.

Hole injection between the AlGaInP active region and the *p*-type AlGaAs cladding or DBRs in hybrid laser heterostructures is complicated by growth difficulties associated with complete group V changeout and reversed valence band offsets at the As/P interfaces, and relatively high *n*-type background carrier concentrations typical in $(Al_yGa_{1-y})InP$, necessitating *p* doping in the AlGaInP to enhance hole transport. Here we modify the cavity design relative to previous reports to overcome these difficulties and eliminate the need for Mg or Zn doping in the AlGaInP, by incorporating As/P transition layers at the interfaces and reducing the *n*-type background concentrations in the active region barrier layers. Our choice for the transition layer is strained $AlAs_xP_{1-x}$ (x graded between ~0.5 and 1.0), which provides improved interface quality due to continuous grading of the group V sublattice composition, amenability to C doping, and the possibility of more continuous grading of the band offsets at the cavity-DBR interface. This latter point is illustrated in Fig. 1, showing the dependence of the $AlAs_yP_{1-y}(y \leqslant 0.5)$ band edges on composition x, according to the best available data.[10–12] The relative positions of the $Al_xGa_{1-x}As$ and $(Al_yGa_{1-y})_{0.5}In_{0.5}P$ band edges are also given. By using an appropriate intermediate

[a]Electronic mail: rpschne@sandia.gov

Downloaded¬29¬Oct¬2004¬to¬129.82.229.173.¬Redistribution¬subject¬to¬AIP¬license¬or¬copyright,¬see¬http://apl.aip.org/apl/copyright.jsp

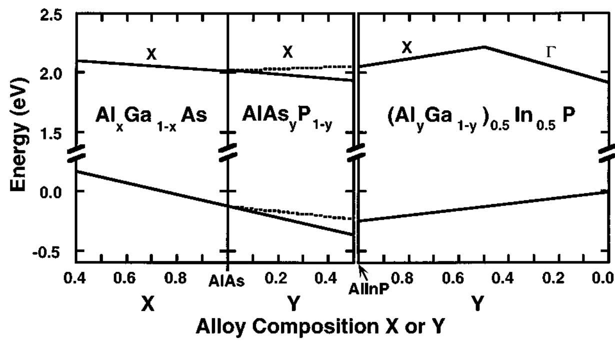

FIG. 1. Conduction and valence band edges for $Al_xGa_{1-x}As$, $AlAs_yP_{1-y}$, and $(Al_yGa_{1-y})_{0.5}In_{0.5}P$ alloys used in the red VCSEL structure. For $AlAs_yP_{1-y}$, the dependence represented by the solid line is from Refs. 10 and 11, while the dashed line is from Ref. 12. Strain is not accounted for in the representation.

$AlAs_yP_{1-y}$ composition, the valence band offset between AlAs and AlGaInP can be graded in a pseudocontinuous manner for all $(Al_yGa_{1-y})InP$ compositions in the range $y=0.5-1.0$,[8–10] and this layer may even contribute to improved carrier confinement. The small tensile strain can be accommodated in a sufficiently thin layer ($\leqslant 10$ nm) to avoid relaxation.

The performance of several EEL heterostructures, grown with and without AlAsP transition layers, and with different AlGaInP barrier layer composition and doping, were compared to determine their suitability for VCSELs. Key laser characteristics include the highest possible carrier confinement, as evidenced by the T_0 in EELs,[13] for reduced carrier leakage at the elevated temperature present in VCSEL optical cavities,[14,15] as well as low threshold current densities. The structures and resulting device data are given in Table I. Included is a conventional all-AlGaInP single quantum well laser diode, (a), employing AlInP cladding layers, and *p*-type doping using Mg for the greatest possible carrier confinement.[6,16] This structure yields the lowest threshold current density, $J_{TH} \leqslant 250$ A/cm^2 (typical), and highest characteristic temperature, $T_0 = 163$ K in the temperature range 20–50 °C. The latter value is, to our knowledge, the highest T_0 ever measured in AlGaInP single quantum well red laser diodes. Replacing the AlInP cladding with AlGaAs typically results in significantly degraded performance, samples (b) and (c). In this case Zn doping on the *p*-side of the junction in the AlGaInP spacer layer is advantageous in improving hole transport across the AlGaAs–AlGaInP interfaces and compensating the relatively high *n*-type backgrounds in the AlGaInP. Some improvement in the laser threshold is observed with the inclusion of the AlAsP transition layer, (c). However, for both samples (b) and (c) the characteristic temperatures T_0 are much lower than for the all-AlGaInP heterostructure, with $T_0 \sim 40-80$ K. These data suggest enhanced carrier leakage into the low-band gap AlGaAs cladding layers, an effect which may also account in part for the higher thresholds in the hybrid lasers. Such leakage can be partly compensated for by including a multiple quantum well active region, as in sample (d). Additional modifications for sample (d) that further reduce the necessity for *p*-doping in the $(Al_yGa_{1-y})_{0.5}In_{0.5}P$ spacer layer include a reduction in the Al mole fraction in the layers to $y \sim 0.5$ to reduce the *n*-type background concentrations while still providing for a large direct band offset at the QWs, and a reduction in the spacer layer thickness commensurate with the additional MQW active region thickness. For this sample, the threshold current density is ~ 330 A/cm^2/QW, much lower than observed in the previous hybrid samples. The T_0 could not be measured due to experimental limitations. Nevertheless, to our knowledge this is the first demonstration of electrically injected lasing in an AlGaInP-based red laser diode employing C as the sole *p*-type dopant.

This approach was next used in AlGaInP/AlGaAs red VCSELs. A schematic of the epitaxial structure and the VCSEL geometry is given in Fig. 2. The optical cavity is 1 λ thick, and contains four 6 nm thick $Ga_{0.44}In_{0.56}P$ strained quantum wells separated by 6 nm thick $(Al_{0.5}Ga_{0.5})_{0.5}In_{0.5}P$ barriers. 10 nm thick $AlAs_xP_{1-x}$($x \geqslant 0.5$) strained transition layers (doped to $n,p \sim 2 \times 10^{18}$ cm^{-3} with Si and C on the respective sides of the junction) are placed on either side of the active region.

Light–current *(L–I)* characteristics for two short-cavity devices, tested under continuous-wave conditions at room temperature, are shown in Fig. 3. At 675 nm, the peak cw output power is 0.83 mW, nearly 15 times greater than the previous best observed in a 670 nm band etched air post structure grown with an extended AlGaInP optical cavity,[2] and nearly three times higher than the previous best observed

TABLE I. Structural parameters for AlGaInP-based broad-area red edge-emitting lasers, and corresponding measurements. For each laser, the cladding layers are ~0.9 μm thick, and the quantum well(s) are surrounded by $(Al_{0.5}Ga_{0.5})_{0.5}In_{0.5}P$ barrier layers and 100 nm thick $(Al_yGa_{1-y})_{0.5}In_{0.5}P$ spacer layers as described in Ref. 6. All lasers were cleaved into 50 μm×800 μm bars and were tested *p*-side up at room temperature under pulsed conditions.

Sample	Cladding composition and doping	Active region (QWs)	$(Al_yGa_{1-y})_{0.5}In_{0.5}P$ spacer composition and doping	Transition layer	J_{th} (A/cm^2/QW) (pulsed)	T_0 (K) (for $T \leqslant 50$ °C)
a	AlInP:Mg	1	$y=0.75$; undoped	N/A	260	163
b	AlGaAS:C	1	$y=0.75$; Zn doped	None	620	46
c	AlGaAS:C	1	$y=0.75$; Zn doped	AlAsP:C	440	74
d	AlGaAs:C	3	$y=0.5$; undoped	AlAsP:C	330[a]	b

[a]Laser bar is 100 μm×515 μm.
[b]T_0 could not be measured due to experimental limitations.

Downloaded¬29¬Oct¬2004¬to¬129.82.229.173.¬Redistribution¬subject¬to¬AIP¬license¬or¬copyright,¬see¬http://apl.aip.org/apl/copyright.jsp

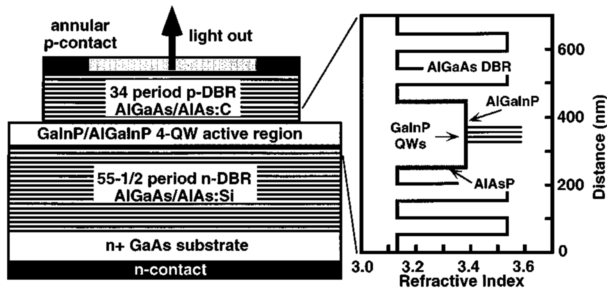

FIG. 2. Schematic of the AlGaInP/AlGaAs red VCSEL etched air post structure, including refractive index profile through the optical cavity. The optical cavity is 1λ thick, and there are 55 1/2 DBR pair on the bottom, and 34 pair on top.

from a 670 nm band gain-guided planar-implanted VCSEL with the same extended-cavity epitaxial design.[3] (It should be noted that these previous devices suffered somewhat from lower external efficiency due to higher output coupler reflectivity and lower total gain, with three QWs rather than the four used here). In addition, the threshold voltage of 2.2 V observed here is significantly lower than the previous best of 2.5 V[2,3] and the voltage remains below 3 V up to rollover. The reduction in the operating voltage in these devices relative to previous red VCSELs despite very similar DBR design and doping may be related to the improved cavity/DBR interface grading scheme. At somewhat longer wavelengths, higher powers and operating efficiencies are achieved as the gain offset with respect to the cavity resonance compensates for device heating.[15] Also shown in Fig. 3 is an $L-I-V$ characteristic for a 15 μm device emitting at 690 nm, exhibiting a peak cw output power of 2.4 mW and a peak power conversion (wallplug) efficiency of 9%. Even further improvements in the device performance have been realized[17] using similar epitaxial structures in planar-implanted geometries which provide better thermal characteristics.[3]

The improved performance of these short-cavity red VCSELs relative to previous structures employing an extended 8 λ thick optical cavity is due in part to reduced free-carrier absorption loss, improved electrical and thermal conductivity of the AlGaAs alloys placed in closer proximity to the active region, and tighter control of the injected current pathway arising from the relative ease with which the AlGaAs materials can be etched closer to the active region. In addition, the ability to use C as the sole p dopant allows a more precise and stable doping profile in the structure. However, the data in Table I suggest tradeoffs between the previous extended cavity and the present short-cavity approaches: The schemes used to eliminate p doping in the AlGaInP and achieve a 1λ optical cavity in the present work give rise to increased carrier leakage (lower T_0) in EELs, and one expects these problems to be exacerbated under the more severe operating conditions present in the VCSEL. A compromise design may yield still more efficient devices.

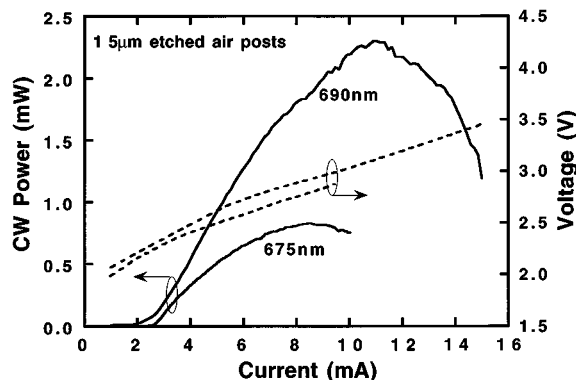

FIG. 3. Room-temperature, cw light–current $(L–I)$ (solid lines) and current–voltage $(I-V)$ (dashed lines) characteristics from 15 μm diameter etched air post red VCSELs employing the 1λ optical cavity design. Data are presented for devices emitting at 675 and 690 nm, corresponding to different gain offset with respect to the cavity resonance.

In summary, we have investigated a modified epitaxial design in AlGaInP/AlGaAs red VCSELs to allow more straightforward implementation of short (1λ) optical cavities and take better advantage of the benefits of AlGaAs in the device structure, including the use of C as the sole p-type dopant. Red (670–690 nm) VCSELs fabricated into simple etched air posts operate cw at room temperature with a peak output power as high as 2.4 mW (at 690 nm), threshold voltage of 2.2 V, and peak wallplug efficiency of 9%, all new performance standards for etched air post red VCSEL diodes.

The authors acknowledge useful discussions with W. W. Chow, T. J. Drummond, G. R. Hadley, and J. Y. Tsao, and technical assistance from S. A. Samora and J. Nevers. This work was supported by the U.S. Department of Energy under Contract No. DE-AC04-94AL85000.

[1] See, for example, J. Quantum Electron. **QE-29**, 1844 (1993), and references therein.
[2] J. A. Lott, R. P. Schneider, Jr., K. D. Choquette, S. P. Kilcoyne and J. J. Figiel, Electron. Lett. **29**, 1693 (1993).
[3] R. P. Schneider, Jr., K. D. Choquette, J. A. Lott, K. L. Lear, J. J. Figiel, and K. J. Malloy, IEEE Photonics Technol. Lett. **6**, 313 (1994).
[4] T. F. Keuch and E. Veuhoff, J. Cryst. Growth **68**, 148 (1984).
[5] P. Unger, G.-L. Bona, R. Germann, P. Roentgen, and D. J. Webb, IEEE J. Quantum Electron. **QE-29**, 1880 (1993).
[6] R. P. Schneider, Jr. and J. A. Lott, Appl. Phys. Lett. **63**, 917 (1993).
[7] R. P. Schneider, Jr., J. A. Lott, K. D. Choquette, S. P. Kilcoyne, and J. J. Figiel, Proceedings of the 1993 Fall Meeting of the Materials Research Society, Boston, MA, 1993, paper M2.3.
[8] B. T. Cunningham, L. J. Guido, J. E. Baker, J. S. Major, N. Holonyak, Jr., and G. E. Stillman, Appl. Phys. Lett. **55**, 687 (1989).
[9] R. P. Schneider, Jr., J. A. Lott, K. L. Lear, K. D. Choquette, S. P. Kilcoyne, and J. J. Figiel, J. Cryst. Growth **145**, 838 (1994).
[10] A. Ichii, Y. Tsou, and E. Garmire, J. Appl. Phys. **74**, 2112 (1993).
[11] J. Tersoff, Phys. Rev. B **30**, 4874 (1984).
[12] W. A. Harrison, J. Vac. Sci. Technol. **14**, 1016 (1977).
[13] D. P. Bour, D. W. Treat, R. L. Thornton, R. S. Geels and D. F. Welch, IEEE J. Quantum Electron. **QE-29**, 1337 (1993).
[14] J. W. Scott, S. W. Corzine, D. B. Young, and L. A. Coldren, Appl. Phys. Lett. **62**, 1050 (1993).
[15] D. B. Young, J. W. Scott, F. H. Peters, M. L. Majewski, B. J. Thibeault, S. W. Corzine, and L. A. Coldren, IEEE J. Quantum Electron. **QE-29**, 2013 (1993).
[16] D. P. Bour, D. W. Treat, K. J. Beernink, B. S. Kursor, R. S. Geels, and D. F. Welch, IEEE Photonics Technol. Lett. **6**, 128 (1994).
[17] M. H. Crawford, R. P. Schneider, Jr., K. D. Choquette, K. L. Lear, S. P. Kilcoyne, and J. J. Figiel, IEEE Photon. Technol. Lett. (in press).

Downloaded¬29¬Oct¬2004¬to¬129.82.229.173.¬Redistribution¬subject¬to¬AIP¬license¬or¬copyright,¬see¬http://apl.aip.org/apl/copyright.jsp